

## Article

# Cytotoxic Effect of Amyloid- $\beta$ 1-42 Oligomers on Endoplasmic Reticulum and Golgi Apparatus Arrangement in SH-SY5Y Neuroblastoma Cells

José J. Jarero-Basulto <sup>1,†</sup>, Yadira Gasca-Martínez <sup>2,†</sup>, Martha C. Rivera-Cervantes <sup>1</sup>, Deisy Gasca-Martínez <sup>3</sup>, Nidia Jannette Carrillo-González <sup>2</sup>, Carlos Beas-Zárate <sup>4</sup> and Graciela Gudiño-Cabrera <sup>2,\*</sup>

- <sup>1</sup> Cellular Neurobiology Laboratory, Cell and Molecular Biology Department, University Center of Biological and Agricultural Sciences (CUCBA), University of Guadalajara, Zapopan 45220, Mexico; jose.jarero@academicos.udg.mx (J.J.J.-B.); mrivera@academicos.udg.mx (M.C.R.-C.)
- <sup>2</sup> Development and Neural Regeneration Laboratory, Cell and Molecular Biology Department, University Center of Biological and Agricultural Sciences (CUCBA), University of Guadalajara, Zapopan 45220, Mexico; yadira.gasca3953@alumnos.udg.mx (Y.G.-M.); nidia.carrillo@academicos.udg.mx (N.J.C.-G.)
- <sup>3</sup> Behavioral Analysis Unit, Neurobiology Institute, Campus UNAM, Juriquilla 76230, Mexico; gasca@inb.unam.mx
- <sup>4</sup> Neurobiotechnology Laboratory, Cell and Molecular Biology Department, University Center of Biological and Agricultural Sciences (CUCBA), University of Guadalajara, Zapopan 45220, Mexico; carlosbeas55@gmail.com
- \* Correspondence: graciela.gudino@academicos.udg.mx; Tel.: +52-33-37771150
- † These authors contributed equally to this work.

**Abstract:** Amyloid- $\beta$  oligomers are a cytotoxic structure that is key for the establishment of the beginning stages of Alzheimer's disease (AD). These structures promote subcellular alterations that cause synaptic dysfunction, loss of cell communication, and even cell death, generating cognitive deficits. The aim of this study was to investigate the cytotoxic effects of amyloid- $\beta$ 1-42 oligomers (A $\beta$ O) on the membranous organelles involved in protein processing: the endoplasmic reticulum (ER) and Golgi apparatus (GA). The results obtained with 10  $\mu$ M A $\beta$ O in SH-SY5Y neuroblastoma cells showed that oligomeric structures are more toxic than monomers because they cause cell viability to decrease as exposure time increases. Survivor cells were analyzed to further understand the toxic effects of A $\beta$ O on intracellular organelles. Survivor cells showed morphological alterations associated with abnormal cytoskeleton modification 72–96 h after exposure to A $\beta$ O. Moreover, the ER and GA presented rearrangement throughout the cytoplasmic space, which could be attributed to a lack of constitutive protein processing or to previous abnormal cytoskeleton modification. Interestingly, the disorganization of both ER and GA organelles exposed to A $\beta$ O is likely an early pathological alteration that could be related to aberrant protein processing and accumulation in AD.

**Keywords:** amyloid- $\beta$ ; amyloid- $\beta$ 1-42 oligomers; cytoskeleton modification; endoplasmic reticulum rearrangement; Golgi apparatus rearrangement



**Citation:** Jarero-Basulto, J.J.; Gasca-Martínez, Y.; Rivera-Cervantes, M.C.; Gasca-Martínez, D.; Carrillo-González, N.J.; Beas-Zárate, C.; Gudiño-Cabrera, G. Cytotoxic Effect of Amyloid- $\beta$ 1-42 Oligomers on Endoplasmic Reticulum and Golgi Apparatus Arrangement in SH-SY5Y Neuroblastoma Cells. *NeuroSci* **2024**, *5*, 141–157. <https://doi.org/10.3390/neurosci5020010>

Academic Editor: François Ichas

Received: 19 March 2024

Revised: 28 April 2024

Accepted: 30 April 2024

Published: 7 May 2024



**Copyright:** © 2024 by the authors. Licensee MDPI, Basel, Switzerland. This article is an open access article distributed under the terms and conditions of the Creative Commons Attribution (CC BY) license (<https://creativecommons.org/licenses/by/4.0/>).

## 1. Introduction

In Alzheimer's disease (AD), the abnormal processing of amyloid precursor proteins in several membranous organelles can produce amyloid peptides (A $\beta$ ) with particular features and lengths. The main neurotoxic isoforms include A $\beta$ 1-40 and A $\beta$ 1-42, both with important aggregative properties. An irregular production of these isoforms enhances their accumulation and has intracellular effects. A $\beta$ 1-40 and A $\beta$ 1-42 have been mostly found in vascular and brain lesions, respectively [1,2]. A $\beta$ 1-42 peptides can self-associate and rise to small, toxic, and non-fibrillary A $\beta$  oligomers, and the number of oligomers is correlated with the extent of cognitive impairment [2,3]. In vitro and in vivo studies have demonstrated that soluble A $\beta$ 1-42 oligomers (A $\beta$ O) are highly toxic to neurons, even

more so than monomers (A $\beta$ Ms) and fibrillary structures [4,5]. This has led researchers to consider A $\beta$ Os as a causal factor in early AD pathogenesis [4–6].

Although the role of A $\beta$ Os in AD pathogenesis is controversial, several studies suggest that they induce early cytotoxicity through different cellular and biochemical mechanisms. Among the proposed damage mechanisms are membrane permeability alterations, interactions with specific signaling receptors, the loss of Ca<sup>2+</sup> homeostasis, mitochondria and endoplasmic reticulum (ER) dysfunction, the overproduction of free radicals, and the induction of abnormal Tau protein phosphorylation, among many others [7–9]. In recent decades, there has been increased interest in the possibility that A $\beta$  oligomers could be the main cause of early organelle alterations, before high-weight aggregate formation [10,11] and cell death [12–14].

Therefore, it is crucial to investigate the toxic role of A $\beta$ Os in intracellular organelles as a mechanism target involved in AD pathogenesis. Although the underlying mechanisms of A $\beta$ O formation and extracellular accumulation remain unknown, structural alterations of membranous organelles like the ER and Golgi apparatus (GA) could be considered key events in AD, eliciting abnormal protein processing, aggregation onset, and accumulation.

The ER is a membranous organelle involved in protein processing, folding, and trafficking [2,15]. The GA, on the other hand, is involved in the post-translational processing, trafficking, and sorting of proteins from the ER [16–18]. Interestingly, both intracellular organelles exhibit alterations in AD and other neurological disorders. These alterations have been associated with the excessive accumulation of misfolded proteins. This study aimed to investigate the cytotoxic effects of A $\beta$ Os on the ER and GA in the SH-SY5Y neuroblastoma cell line, in order to further understand the early alterations in abnormal protein processing associated with incipient AD pathogenesis.

## 2. Materials and Methods

**In vitro formation of A $\beta$ 1-42 oligomers:** Freeze-dried A $\beta$ 1-42 peptides (AnaSpec, San José, CA, USA) were dissolved in 1,1,1,3,3,3-hexafluoro-2-propanol 1 mM (HFIP) (Sigma-Aldrich, St. Louis, MO, USA) and aliquoted in samples of 100  $\mu$ M. The samples were vacuum centrifuged in a Speed-vac Spd111v (Thermo Fisher Scientific Brand, Waltham, MA, USA) until the solvent evaporated. Next, a thin and colorless film of the stable peptide was taken from the tube bottom. A $\beta$ 1-42 peptides were oligomerized in vitro by adapting conditions previously described by Klein [19]. The samples of A $\beta$ 1-42 peptides were re-suspended in 5 mM dimethyl sulfoxide anhydride (DMSO) (Sigma-Aldrich, St. Louis, MO, USA) and diluted in phosphate-buffered saline 1X (PBS-1X) to a concentration of 10  $\mu$ M. The mix was incubated at 37 °C for up to 0, 3, 6, 12, and 24 h for oligomerization kinetics. As in previous works [20,21], SDS-PAGE and Western blotting (WB) were used to confirm and monitor the A $\beta$ O aggregate formation, as referenced later.

**SH-SY5Y cell culture and A $\beta$ O treatment:** SH-SY5Y human neuroblastoma cells were obtained from American Type Culture Collection (ATCC CRL-2266) (Manassas, VA, USA) and cultured in Dulbecco's Modified Eagle Medium-F12 (DMEM-F12) (Invitrogen Life Technologies-GIBCO, Carlsbad, CA, USA) supplemented with 10% (*v/v*) Fetal Bovine Serum (FBS) (Invitrogen), 2 mM L-glutamine, 100 U/mL penicillin, and 100  $\mu$ g/mL streptomycin. The cells were kept in a humidified atmosphere of 5% CO<sub>2</sub> at 37 °C, and the culture medium was replaced every three days. The cells at 70–80% confluence were exposed to 10  $\mu$ M A $\beta$ Os suspended in DMEM-F12/FBS 2% and incubated for 3, 6, 12, 24, 48, 72, and 96 h. Seventy-two hours after A $\beta$ O incubation, the treatment was changed and maintained for 96 h. At the end of each incubation period, the cells were washed in PBS-1X, pH 7.4, and processed for the different assays.

**MTT assay:** The MTT (3-(4, 5-dimethylthiazol-2-yl)-2,5-diphenyltetrazolium bromide, Sigma-Aldrich, St. Louis, MO, USA) assay was used to evaluate the cell viability. This method is used to determine a healthy cell's ability to produce formazan from the cleavage of the MTT tetrazolium ring (the color changes from yellow to blue) [22]. Briefly, 96-well plates with SH-SY5Y cells non-exposed and exposed to A $\beta$ Os were incubated in fresh

DMEM-F12 containing 0.5 mg/mL MTT for 3 h at 37 °C. Thereafter, the MTT medium was discarded, and the cells were incubated in DMSO (Sigma-Aldrich, St. Louis, MO, USA) to dissolve the formazan crystals. Finally, the intensity of MTT products was read at 570 nm using a microplate spectrophotometer (Multiskan-Go, Thermo Scientific, Waltham, MA, USA).

**Immunocytochemistry and microscopy:** SH-SY5Y cell cultures exposed and non-exposed to A $\beta$ O were processed for triple-labeling immunofluorescence. Initially, cells were fixed with 2% paraformaldehyde at room temperature (RT) for 15 min and permeabilized in 0.1% Triton X-100-PBS (PBS-T). Afterward, cells were blocked in a solution containing 0.1% gelatin and 1.5% FBS in PBS-1X for 20 min at RT. Double labeling with primary antibodies (Table 1) was conducted for 1 h at RT in a humidity chamber. The secondary antibodies corresponding to mouse-IgG and rabbit-IgG were tagged with either fluorescein isothiocyanate (FITC) or tetramethylrhodamine isothiocyanate (TRITC) (Jackson Immuno-Research Laboratories, Inc., West Grove, PA, USA), and simultaneously incubated in PBS-T for 1 h at RT (1:200 dilution). In some experiments, filamentous actin (F-actin) was evaluated by counterstaining with rhodamine phalloidin, a fluorescent phalloxin specific to F-actin (Invitrogen Molecular Probes, Eugene, OR, USA). The Hoechst-33258 fluorescent nuclear marker was also included in triple labeling (Invitrogen-Molecular Probes). Immunolabeled samples were analyzed with a Nikon Eclipse-80i epifluorescence microscope (Nikon Corp., Tokyo, Japan). Samples were observed through 20 $\times$  and 40 $\times$  Plan-Fluor Lens and the images were obtained and recorded using a Nikon digital sight-DG-Ri1 camera and the Nikon NIS-Elements AR-3.1-SP7 software.

**Table 1.** Antibodies and fluorescent markers employed.

Antibody	Epitope	Host-Class	Procedure	Reference
Anti- $\beta$ -Amyloid 1-42	1-42 aa	rabbit IgG	IC, WB	Abcam Inc., Waltham, MA, USA
$\alpha$ -Tubulin	$\alpha$ -Tubulin	mouse IgG	IC	Santa Cruz Biotechnology, Inc., Dallas, TX, USA
$\beta$ -Actin	$\beta$ -Actin	mouse IgG	WB	Santa Cruz Biotechnology, Inc., Dallas, TX, USA
RCAS 1	Gly 147	rabbit IgG	IC	Cell Signaling Technology, Danvers, MA, USA
Golgin-97 (CDF4)	Human Golgin-97	mouse IgG	IC, WB	Invitrogen molecular probes, Eugene, OR, USA
Calnexin (C5C9)	Human Calnexin	rabbit IgG	IC, WB	Cell Signaling Technology, Danvers, MA, USA
Organelle	Fluorescent marker	Excitation/emission	Procedure	Reference
Nuclei	Hoechst-33258	350/461	FL	Invitrogen Molecular Probes, Eugene, OR, USA
F-Actin cytoskeleton	Rhodamine-phalloidin	540/565	FL	Invitrogen Molecular Probes, OR, USA

IC: Immunocytochemistry; WB: Western blotting; FL: fluorescence.

**Electrophoresis and immunoblotting analysis of cell extracts:** SH-SY5Y cells exposed and non-exposed to A $\beta$ O were washed with ice-cold PBS-1X, scraped and lysed in radioimmunoprecipitation assay (RIPA) buffer containing a protease inhibitor cocktail (150 mM NaCl, 50 mM Tris, pH 8.0, 1.0% Triton X-100, 0.5% sodium deoxycholate, 1 mM PMSF, 100 mM NaF, 1 mM Na<sub>3</sub>VO<sub>4</sub>, 2  $\mu$ g/mL complete; Roche, IN, USA), and then centrifuged for 10 min at 12,000 $\times$  g. In some experiments, non-exposed cells were treated with 1  $\mu$ g/mL actinomycin-D (at the same times used for A $\beta$ O exposure) to induce cell death and then lysed and processed. The supernatant was collected and the protein content in all samples was determined by the mini-Bradford assay using the Bradford protein assay reagent (Sigma-Aldrich). For each sample, 30  $\mu$ g of protein was diluted 1:1 in 2X sample buffer (Tris-HCL 100 mM pH 6.8, sodium dodecyl sulfate (SDS) 4%, bromophenol blue 0.2%,  $\beta$ -mercapto-ethanol 5%, and glycerol 20%) and boiled for 5 min at 95 °C. All samples were separated by electrophoresis on 10% SDS-polyacrylamide gel (SDS-PAGE) and transferred

to a nitrocellulose membrane for immunoblotting analysis. Nitrocellulose membranes containing the transferred proteins were blocked in dried 5% non-fat milk in PBS-0.1%-Tween 20 (PBS-Tw) overnight at 4 °C and processed for immunolabeling with primary antibodies (Table 1), diluted in PBS-Tw, incubated at RT for 1 h, and then washed. After that, incubation with the peroxidase-conjugated secondary antibody corresponding to either mouse or rabbit (1:30,000; Jackson Immuno-Research, Laboratories, Inc., West Grove, PA, USA) was performed for 1 h, diluted in PBS-Tw. Protein reactivity was visualized using the WesternSure ECL substrate (LI-COR, Inc., Lincoln, NE, USA) and developed on autoradiography films (Amersham hyperfilm ECL; Amersham BioSciences, Buckinghamshire, UK). The band density in the WB were quantified with the Image J program V1.8.0 (<http://rsb.infor.nih.gov/ij>, accessed on 22 May 2023), indicating the same analysis area in each of the captured images (area value calculated in pixels). The values were averaged and compared between samples.

### 3. Results

#### 3.1. A $\beta$ O<sub>s</sub> Assembled In Vitro

Several studies demonstrate that A $\beta$ O toxicity is crucial for the onset of neurodegeneration in AD pathogenesis, causing noxious effects both outside and inside the cell. These effects lead to a series of atypical events that result in slow and progressive cell death in the brain. In this study, we investigated the effect of A $\beta$ O<sub>s</sub> on SH-SY5Y cell viability and intracellular organelles like the ER and GA. To achieve this goal, we designed oligomerization kinetics using A $\beta$ 1-42 synthetic peptides and determined the formation of the A $\beta$ O in vitro by WB (as other works [20,21]) before evaluating its cytotoxicity in SH-SY5Y cell cultures. A $\beta$ O formation was identified at all selected times for the kinetics (Figure 1, from 3 to 24 h). Different distribution patterns and intensities of A $\beta$ 1-42 bands were observed using the specific A $\beta$  antibody. After 3 h of A $\beta$ 1-42 oligomerization induction, a significant increase in the immunoreactive bands corresponding to A $\beta$  tetramers (A $\beta$ T ~18 kDa) and A $\beta$ O<sub>s</sub> (over 45 kDa weight) were detected in the same sample mixture (Figure 1, line 2). A $\beta$ O band immunoreactivity increased over time, while A $\beta$ T bands gradually decreased and eventually disappeared (Figure 1, lines 2–5). In the same assay, A $\beta$ M (~4 kDa) bands were clearly identified before the kinetics of oligomerization at 0 h (line 1). However, they also disappeared when the time increased from 3 to 24 h (lines 2–5). The results showed that A $\beta$ O aggregates could be detected as early as 3 h, but the maximum degree of oligomerization was not found until 24 h later, when the A $\beta$ M and A $\beta$ T pools disappeared completely. Thus, we determined 24 h of oligomerization as a suitable time to acquire the amount of A $\beta$ O necessary to assess the cytotoxic effect on SH-SY5Y cells in subsequent experiments.

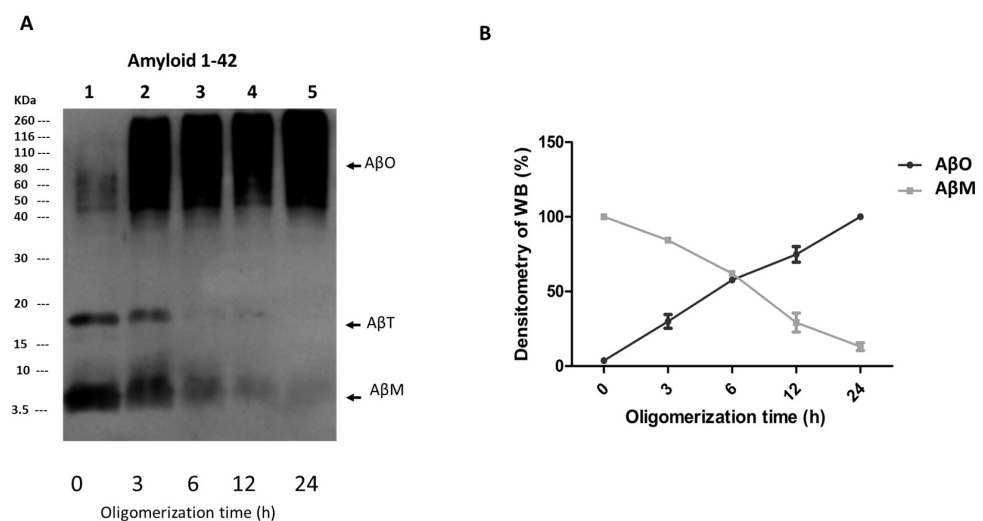


**Figure 1.** Analysis of A $\beta$ 1-42 peptide oligomerization in vitro. A $\beta$ 1-42 peptides were assembled in vitro in oligomerization kinetics for 0, 3, 6, 12 and 24 h using Klein's protocol [19]. (A) Oligomerization

samples were analyzed by SDS-PAGE and the different aggregation states of the A $\beta$ 1-42 peptides were detected by WB using the monoclonal antibody anti-A $\beta$ 1-42. The arrows indicate A $\beta$ M (~4 kDa), A $\beta$ T (~18 kDa), and A $\beta$ O (>45 kDa) forms. (B) From three independent experiments, the relative value of immunoreactivity for the anti-A $\beta$ 1-42 antibody in the A $\beta$ O bands was averaged and plotted with respect to the time.

### 3.2. A $\beta$ O Toxicity in SH-SY5Y Cell Cultures Is Time-Dependent

To check if the A $\beta$ O obtained after 24 h of oligomerization could induce cytotoxicity in SH-SY5Y cells, as many reports suggest [23–25], we analyzed the cell viability 3, 12, 24, 48, 72, and 96 h after exposure to 10  $\mu$ M A $\beta$ O, a concentration previously determined by other authors [26–28]. At the end of the exposure time, we used the MTT reduction assay to evaluate cell viability. The results revealed that 10  $\mu$ M A $\beta$ O decreased cell viability in a time-dependent manner compared with the control group (Figure 2). Although, the tested A $\beta$ O concentration was not lethal to all cells and did not cause intense cell loss (Figure 2A–D). In order to determine whether the decrease in cell population was caused by A $\beta$ O and not only by the presence of A $\beta$ , SH-SY5Y cells were also exposed to 10  $\mu$ M A $\beta$ M under same conditions. In this case, the cells exhibited a slight decrease in their viability percentage (gray bars), but it was not comparable with that of the A $\beta$ O group (white bars). When cells exposed to A $\beta$ O were compared to A $\beta$ M-exposed cells, significant changes were observed in the A $\beta$ O group, with a 50% viability reduction against a 20% decrease observed in the A $\beta$ M group from 72 h to 96 h (E and F), confirming the limited toxicity of A $\beta$ M. As a positive death control, SH-SY5Y cells were treated with 1  $\mu$ g/mL actinomycin-D (textured bars) for the same times used previously. The observed decrease in cell viability was more significant than in the A $\beta$ O group. In addition, SH-SY5Y cells exposed to PBS-1X + DMSO were used as a viability control. These findings suggest that A $\beta$ O toxicity leads to an increase in cell death in SH-SY5Y cell cultures, which correlates with previous observations by different research groups, supporting the hypothesis that A $\beta$ O plays a toxic role in AD pathogenesis. However, we found that A $\beta$ O exposure was not lethal for the cells. Even 72 to 96 h after exposure, around 50% of the cells managed to survive, indicating that A $\beta$ O caused alterations at the subcellular level that led to slow cell death, similar to what occurs in AD.

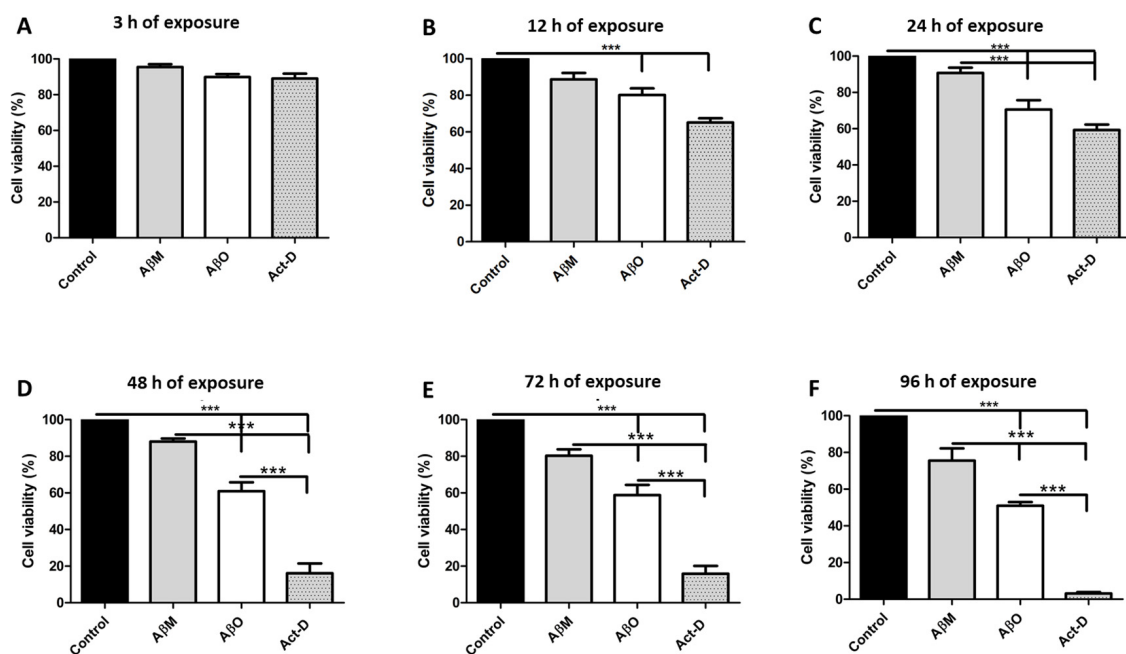


**Figure 2.** A $\beta$ O toxicity is time-dependent. The viability of SH-SY5Y cells following exposure to 10  $\mu$ M A $\beta$ O for different times (3, 12, 24, 48, 72, 96 h) was evaluated by an MTT assay. Following A $\beta$ O exposure,

the viability of SH-SY5Y cells decreased in a time-dependent manner (white bars) compared with non-exposed cells (control group, black bars) (A–F). A 50% cell reduction was observed from 72 h ((E), white bar) to 96 h ((F), white bar). In the group exposed to A $\beta$ M (10  $\mu$ M), only a 20% decrease in cell viability was observed at 96 h (gray bars). SH-SY5Y cells exposed to PBS-1X + DMSO and 1  $\mu$ g/mL actinomycin-D (Act-D, textured bars) were used as viability and cytotoxicity control groups, respectively. The rate of MTT reduction was normalized with respect to the control. Differences between groups were significant according to one-way ANOVA and Tukey statistical analysis (\*\* $p < 0.001$ ).

### 3.3. A $\beta$ O<sub>s</sub> Induce Tubulin and Actin Cytoskeleton Modifications in SH-SY5Y Cells

Previous studies have reported significant cytoskeletal alterations when cells are treated with A $\beta$  [29,30]. In this study, we examined the cytoskeleton of survivor SH-SY5Y cells by immunofluorescence with the  $\alpha$ -tubulin antibody and rhodamine-phalloidin specific to F-actin after 72 h of exposure to A $\beta$ O<sub>s</sub> to determine whether A $\beta$ O<sub>s</sub> toxicity causes subcellular structural alterations that support early AD pathogenesis. We compared the distribution to that of non-exposed cells labeled against A $\beta$ O<sub>s</sub>-exposed cells (Figure 3, red channel). We found that the tubulin cytoskeleton of A $\beta$ O<sub>s</sub>-exposed cells had a different distribution and exhibited morphological modifications characterized by an elongated form and slightly wavy processes (Figure 3B, arrow). These changes were associated with an abnormal microtubule (MT) distribution promoted by A $\beta$ O<sub>s</sub>, since they were not observed in non-exposed cells that preserved the normal radial distribution of a tubulin cytoskeleton (Figure 3A, asterisk).

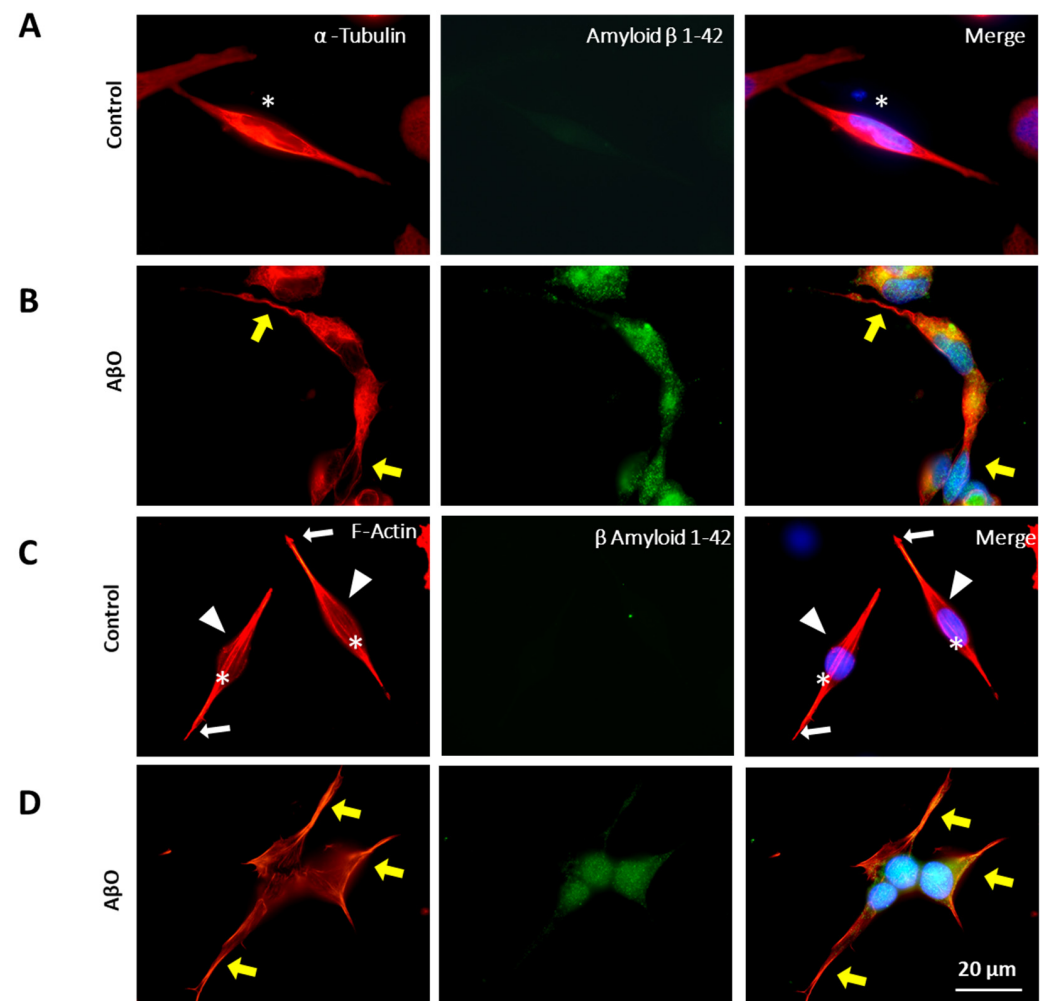


**Figure 3.** A $\beta$ O<sub>s</sub> induce tubulin and F-actin cytoskeleton modifications in SH-SY5Y cells. (A) Control SH-SY5Y cells exhibited a normal radial distribution of the tubulin cytoskeleton (asterisk) and (C) F-actin

cytoskeleton in the immediate vicinity of the plasma membrane (arrowheads), and focal adhesions (small white arrows) and stress fibers with filiform or spindle morphology (asterisks) were also observed. (B) A $\beta$ O-exposed cells showed an elongated form and developed slightly wavy processes due to the modification of microtubule distribution (yellow arrow). (D) Large and thin cytoplasmic processes, irregular plasma membrane lobulations, and a decrease in stress fibers were observed when the F-actin cytoskeleton distribution was altered (yellow arrows). No nucleus alteration was found in the analyzed cells (merge). Scale bars in all panels: 20  $\mu$ m. The panels display the same combination of labels utilized for triple-labeling immunofluorescence by combining A $\beta$  antibody (green channel), Hoechst-33258 (blue channel), and  $\alpha$ -tubulin antibody or rhodamine-phalloidin (red channel).

In the same way, the F-actin cytoskeleton adopted a different distribution, forming large and thin cytoplasmic processes, lobulations on the plasma membrane, and a decrease in stress fibers (Figure 3D, yellow arrows) in A $\beta$ O-exposed cells. In contrast, non-exposed cells showed a normal distribution of the F-actin cytoskeleton with a cortical filamentous arrangement in the immediate vicinity of the plasma membrane (arrowheads), focal adhesions (small white arrows), and stress fibers with filiform or spindle morphology (asterisks), all of which are typical characteristics of SH-SY5Y cells (Figure 3C). Anti- $\beta$ -amyloid 1–42 antibody was used to prove A $\beta$ O cell exposure *in vivo*, before the cell fixation process. Curiously, we observed that the presence of A $\beta$ O in the extracellular space seemed to be associated with the plasma membrane, but we did not investigate this finding further.

### 3.4. A $\beta$ O Induce Endoplasmic Reticulum and Golgi Apparatus Rearrangements in SH-SY5Y Cells

One of the main causes of abnormal protein processing in AD and other pathologies is thought to be the early modification of membranous organelles including the ER and GA. To further study the effects of A $\beta$ O toxicity on SH-SY5Y cells, we investigated whether the organelles were altered early due to extracellular stimulation by A $\beta$ O. We analyzed the morphology of the ER in A $\beta$ O-exposed cells after 72 h by monitoring calnexin, an important integral protein [31]. Our analysis was carried out through triple-labeling immunofluorescence utilizing the calnexin antibody and the same combination of labels as that utilized for the cytoskeleton proteins and nucleus. As shown in Figure 4, a large number of cells exhibited ER disorganization that was dispersed throughout the cytoplasmic space (B and D, yellow arrows). In contrast, control cells that were not exposed to A $\beta$ O showed a normal arrangement with a compact form of the ER, located mostly in the vicinity of the perinuclear space (A and C, asterisks). Interestingly, the nucleus hallmarks were never altered, discarding that the ER disorganization was due to cell division or quick cell death (merge). Based on these results, we next examined whether A $\beta$ O could alter calnexin protein expression, producing ER rearrangement. Protein expression was evidenced by immunoblot analysis of cellular extracts from A $\beta$ O-exposed and non-exposed cells. As shown in Figure 4E, cells exposed to A $\beta$ O for 72 h did not show changes in calnexin protein expression, as it was similar to the expression level observed in the control cells (second and first line, respectively).

Additionally, we analyzed GA morphology by monitoring the RCAS1 antibody, which recognizes RCAS1, an important type-III transmembrane protein of this organelle. We conducted this analysis through triple-labeling immunofluorescence with the same combination of labels utilized previously. As shown in Figure 5, the A $\beta$ O-exposed cells exhibited an abnormal anterograde distribution of the GA throughout most of the cytoplasmic space (B, B1, yellow arrows), acquiring a fragmented appearance. Non-exposed cells maintained a compressed morphology with perinuclear localization (A, asterisks). To determine if this rearrangement in the GA could be due to a decrease in the constitutive Golgin-97 protein expression of this organelle, we examined the levels of this protein by immunoblot analysis with the Golgin-97 antibody. As shown in Figure 5C, after 72 h of exposure to

A $\beta$ O, Golgin-97 expression totally disappeared in cell extracts from exposed cultures. In non-exposed cells, ~98 kDa bands corresponding to this protein were observed.

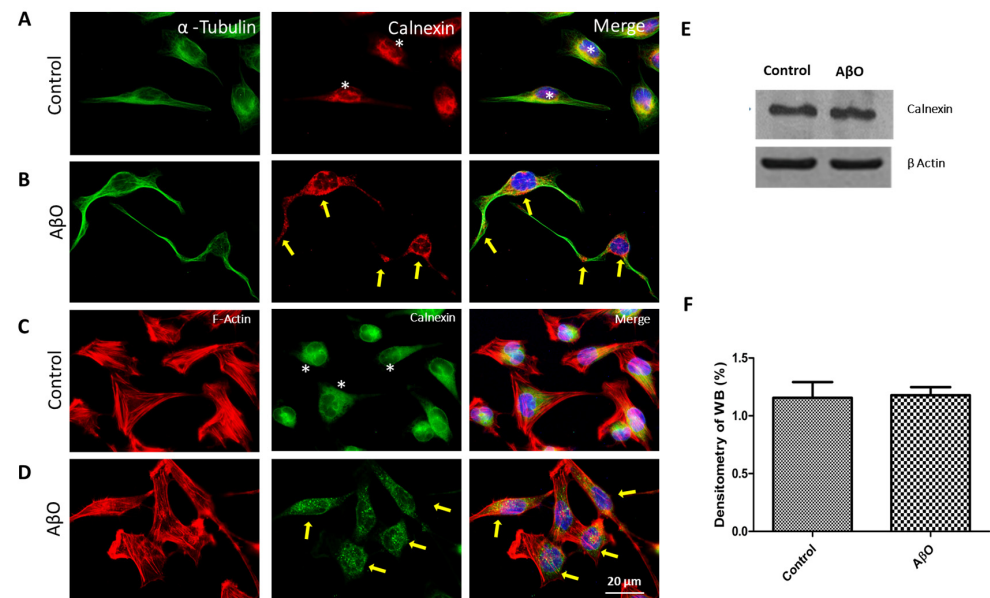


**Figure 4.** Abnormal A $\beta$ O-induced rearrangement of the ER in SH-SY5Y cells. (A,C) SH-SY5Y cells non-exposed to A $\beta$ O (control) exhibit a compact ER distribution around the nucleus (asterisks). (B,D) A $\beta$ O-exposed cells exhibited a dispersed distribution of the ER throughout the cytoplasmic space (yellow arrows). No nucleus alteration was found in the analyzed cells (merge). Scale bars: 20  $\mu$ m. The panels (A,B) display the combination of labels utilized for triple-labeling immunofluorescence by combining  $\alpha$ -tubulin antibody (green channel), calnexin antibody (red channel) and Hoechst-33258 (blue channel). While (C,D) panels display the combination of rhodamine-phalloidin (red channel), calnexin antibody (green channel) and Hoechst-33258 (blue channel). (E) Representative WB evidenced no alterations in calnexin protein expression (as shown in ~90 kDa bands) in both lines, corresponding to total extract from exposed and non-exposed cells.  $\beta$ -actin (~47 kDa bands) was used as a loading control. (F) From three independent experiments, the relative value of immunoreactivity for anti-calnexin antibody in the recognized bands was averaged and plotted. In all panels, the ER was identified with calnexin antibody.

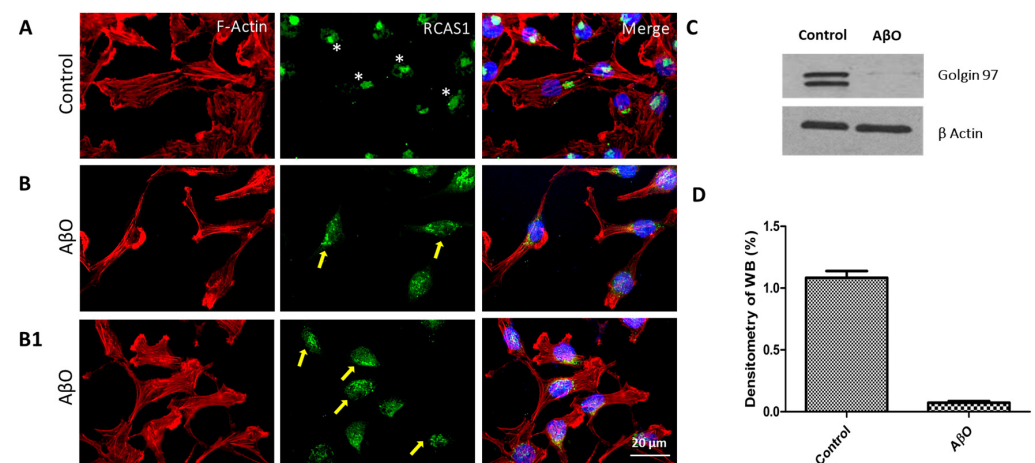


**Figure 5.** Abnormal A $\beta$ O-induced rearrangement of the GA in SH-SY5Y cells. (A) SH-SY5Y cells non-exposed to A $\beta$ O exhibit a normal GA compressed arrangement (asterisks). (B,B1) In A $\beta$ O-exposed cells, a dispersed rearrangement throughout the cytoplasmic space of the GA was evidenced after 72 h

(yellow arrows). All cells were processed for triple immunolabeling, like in previous experiments, the panels display the combination of rhodamine-phalloidin (red channel), RCAS1 antibody (green channel) and Hoechst-33258 (blue channel). No nucleus alteration was found in the analyzed cells (merge). Scale bars in all panels: 20  $\mu\text{m}$ . (C) Representative WB evidenced the disappearance of bands indicative of Golgin-97 expression in A $\beta$ O-exposed cells. In non-exposed cells, ~98 kDa bands corresponding to the same protein were observed.  $\beta$ -actin (~47 kDa bands) was used as a loading control. (D) From three independent experiments, the relative value of immunoreactivity for the anti-Golgin-97 antibody in the recognized bands was averaged and plotted.

#### 4. Discussion

Although A $\beta$  peptide can be present in several different conformations such as monomers, oligomers, protofibrils, and fibrils in the brain tissue from AD patients, in the last decades, *in vitro* and *in vivo* studies have demonstrated that soluble are the most toxic peptide form [4,5]. However, the main toxic contribution of A $\beta$ O to this disease pathogenesis continue to be controversial and not fully understood. It is known that during the amyloidogenic process occurs the formation of several A $\beta$  aggregates with different structural features, and as a consequence of this highly heterogeneous aggregation process, differential toxicity degrees have been reported [32]. For a long time, the fibrillary forms of A $\beta$  were considered key toxic agents in pathogenesis, due their abundance in amyloid plaques in the brains of AD patients and supported by some experimental approaches, where cognitive impairment was associated with synaptic transmission damage and subsequent neuronal cell death [33]. Nevertheless, the most controversial discussion of fibrillary toxicity is the lack of correlation between amyloid plaque burden and the severity of AD [34]. On the other hand, during the amyloidogenic process A $\beta$  oligomers as intermediary forms are also formed, which, contrary to fibrils, have demonstrated a significant correlation with the impairment of learning and memory [3]. Derived from this background, current studies focused on A $\beta$  oligomers highlight that unlike fibrils, A $\beta$ O have structural characteristics that could be involved in their cytotoxicity, e.g., small size, structural content, and high surface hydrophobicity. These features are responsible for generating highly heterogeneous oligomeric aggregates that are complicated to understand. The study of A $\beta$  oligomers represents a complex challenge, but one that opens up the possibility to clarify the origin of AD pathogenesis. Interestingly, Siddiqi and coworkers reported evidence on the differential toxicity of the different A $\beta$  aggregates, highlighting the pathological importance among them and that each one represents [32]. Particularly, in the present work, we limited ourselves to analyzing the cytotoxic effects of a variable population of A $\beta$ O (45 to 250 kDa).

In recent decades, the subcellular alterations caused by A $\beta$ O toxicity have also been studied using cellular models that mimic tissue conditions in AD. The current research is focused on demonstrating the pathological mechanisms of A $\beta$ O toxicity, regardless of its intra- or extracellular location. Various studies have shown that A $\beta$ O aggregates may generate abnormal modifications in distinct subcellular components, disrupting normal cell functioning and leading to synaptic dysfunction and the loss of cell communication [30,35], before to causing cellular death [29,36,37], a situation that might correlate with cognitive impairment in AD.

Particularly, the aim of the present study was to investigate the cytotoxic effects of A $\beta$ O as a pathological stimulus in SH-SY5Y cells, in order to further understand their consequences on the most important membranous organelles involved in protein processing: the ER and GA. To this end, we exposed SH-SY5Y cells to A $\beta$ O aggregates and probed their toxic effects *in vitro*. We found that 10  $\mu\text{M}$  of A $\beta$ O was enough to generate cell death in the cultures. This effect increased over time. Although our findings corroborated the cytotoxic effect of A $\beta$ O, as other research groups have reported previously [38–40], it is important to indicate that cell death did not occur in all cells, and even 96 h after exposure, around 50% of the cells remained alive (Figure 2), at least under our experimental conditions. This could be comparable to the cell death reported for brain cells in cases of

AD, where it is conclusive long after the cellular damage is initiated, until the appearance of typical injuries of this disease [41,42]. According to our hypothesis, A $\beta$ O<sub>s</sub> alter the structure of organelles shortly after they are exposed. These alterations may be incipient changes that in the long term could cause serious damage to cell functionality and, ultimately, neuronal death. Therefore, the abnormal mechanisms triggered by A $\beta$ O<sub>s</sub> might be responsible for the onset of slow cell death. However, we cannot ensure this fact with these results.

Many researchers consider cytoskeleton alterations caused by the presence of different kinds of A $\beta$  aggregates to be the beginning of cognitive impairment in AD [43,44], as is involved in the permanent disruption of neuronal connections, causing neurite breakage and synaptic loss [45–48]. The cytoskeleton is an important cellular component with versatile functionality. It is involved in several vital processes such as cell shape maintenance, intracellular transport, motility, cell division, adhesion, and preservation, among others. Previous studies reported that the alteration of the cytoskeleton is a common hallmark of different diseases, including AD [29]. In this study, we found that exposure to A $\beta$ O<sub>s</sub> altered the normal spindle-like morphology of survivor SH-SY5Y cells after 72 h, probably as an effect that occurs before cell death. The survivor cells changed to show a reduced somatic compartment accompanied by long and wavy projections (Figure 3B). Although the action mechanism was not characterized, these changes were attributed to MT alterations as part of the tubulin cytoskeleton arrangement, which changed its radial distribution to abnormal compact cellular processes. Previous studies using cell models with A $\beta$  exposure have also found an abnormal distribution of MTs [11,29]. Cytoskeletal disintegration is an event often observed in apoptotic cells and implicates an evident morphological cell change. Interestingly, we did not find evidence of MT depolymerization or nuclear component alteration; hence, this effect seems to be independent of an incipient apoptotic process. We highlight that the MT network alteration is seemingly not enough to cause a significant loss of cell viability, at least after 96 h of A $\beta$ O<sub>s</sub> exposure. However, it could be further evaluated.

Qu and colleagues hypothesized that A $\beta$  can activate pathways that alter MT function but also promote post-translational modifications (PTMs) [11]. Tubulin is a protein that can undergo a series of PTMs (e.g., detyrosination, polyglutamylation, and acetylation) that affect its functionality and MT stability [49,50], triggering cellular stress. It has been shown in earlier studies that detyrosinated tubulin can induce changes in MTs. This finding was obtained using experimental models that included A $\beta$  or Tau protein in neuronal and glial cells, respectively, although with different reactions [51,52]. While A $\beta$  induced stable detyrosination [51], Tau induced a selective reduction in detyrosination [53], but in both cases, the MT alteration affected cell communication. Although the mechanism involved in MT alteration is unclear, it has been associated with Rho effectors because they can act in independent roles in MTs or the actin cytoskeleton [54], due to its differential regulation or its combination with other formins in the same cell. This evidence suggests that A $\beta$  and Tau toxicity, with different cell localizations and action pathways, can contribute to MT modification and have similar abnormal effects on cells.

Similar to our data on tubulin, we found a considerable change in the F-actin cytoskeleton when the SH-SY5Y cells were exposed to A $\beta$ O<sub>s</sub>. The typically filamentous-type arrangement and submembrane cortical localization [55] of these components were modified and adopted an abnormal distribution that contributed to the development of elongated and thin cytoplasmic processes, plasmatic membrane lobulations, and a decrease in stress fibers in the majority of survivor cells (Figure 3D). Interestingly, in this case, the morphological changes were attributed to the decrease in the total polymerized pool of F-actin protein, since the intensity of the fibrillary phalloidin–rhodamine signal was notably reduced and, consequently, changed its distribution after A $\beta$ O<sub>s</sub> exposure. It should be noted that the F-actin cytoskeleton participates in several physiological functions that support neuronal connectivity [56,57]. Therefore, its alteration seems to be associated with abnormal changes linked to cellular communication deficiency, a common failure in AD. Accordingly, Ma et al. [58] reported that in primary culture hippocampal neurons, A $\beta$ O<sub>s</sub> induced F-actin depolymerization and degradation through Tiam1/Rac/PAK pathway activation, causing

a decrease in dendrites and synaptic deficits. Nam and colleagues [59] demonstrated that exposing N2a cells to A $\beta$ O<sub>s</sub> altered the F-actin cytoskeleton, directly affecting the GTPase/formin family and the Wnt pathway. Interestingly, Torres-Cruz and colleagues [52] demonstrated that Tau protein expression in cultured C6 glial cells altered the organization of the F-actin cytoskeleton and caused abnormal lobulations in the membrane. These authors also explained that the effects were initiated by the abnormal distribution of the tubulin cytoskeleton induced by Tau protein, which produced the release of microtubule-bound guanine nucleotide exchange factor-H1 (GEF-H1) into the cytoplasm, activating the Rho/GTPase/ROCK pathway responsible for rearranging F-actin [52]. Similar data were also obtained by Qu and colleagues [11] in hippocampal neurons using A $\beta$ O<sub>s</sub> as a toxic stimulus. The MTs were altered after A $\beta$ O<sub>s</sub> exposure in a Rho-mediated manner, suggesting that the mechanism is similar to the one described before for Tau protein in C6 glial cells. In this case, however, the mechanism was initiated by the APP/caspase/RhoA signaling cascade, which is involved in the loss of dendritic spines made of actin.

Although the mechanisms underlying A $\beta$ O<sub>s</sub> toxicity are complex and poorly understood, our data support the evidence that A $\beta$ O<sub>s</sub>, as a pathological stimulus, induce significant alterations in the tubulin and F-actin cytoskeleton, leading to morphological changes that destabilize cell viability. However, further research is needed to fully understand this mechanism.

Abnormal cytoskeleton modification could explain why A $\beta$ O<sub>s</sub> causes significant morphological changes. Furthermore, this alteration could be involved in the distribution and function of intracellular organelles, as has been proposed [11,29]. An increasing body of evidence in both patients and experimental models of AD supports that A $\beta$ O<sub>s</sub> alter the cytoskeleton network, affecting subcellular organelle integrity [20,60,61]. Considering these findings, in the present, study we sought to identify abnormalities in membranous organelles (ER and GA) produced by A $\beta$ O<sub>s</sub> exposure in SH-SY5Y cells. Along with morphological abnormalities, we found that the ER and GA were significantly rearranged after exposure to A $\beta$ O<sub>s</sub>. Particularly, we identified a pattern of dispersion in the ER, which was present throughout the cell cytoplasm (Figure 4B,D). This could be a consequence of abnormal cytoskeleton distribution. As previous data have shown, the integrity of the cytoskeleton is important to maintaining the architecture and dynamics of the ER in cells [62,63]. Therefore, it is important to continue with the characterization of these possible mechanisms of subcellular alterations.

Modifications in the ER have been documented in AD and other neurological disorders. These modifications affect ER function and cause excessive accumulation of misfolded proteins in its lumen, a condition called ER stress [64–66]. ER stress has partly been associated with a significant increase in A $\beta$  formation and accumulation in this organelle [67]. Interestingly, A $\beta$  originates from the abnormal processing of APP, which is present in several membrane organelles, including the ER [68,69]. Although A $\beta$  accumulation may generate internal toxicity through various mechanisms, this peptide is also released and formed extracellularly, where it can cause damage [70–72]; hence, currently, studies on A $\beta$  toxicity are focused on understanding both the intracellular and extracellular effects [73–75].

Different studies have demonstrated that by generating ER stress, A $\beta$ O<sub>s</sub> trigger a series of actions that impact cellular physiology [76,77]. Pannaccione and coworkers reported that PC12 cells exposed to A $\beta$ O<sub>s</sub> exhibited chronic stress in the ER, which resulted in an excessive release of intracellular Ca<sup>+2</sup> and apoptotic cell death [78]. These data are consistent with previous studies where A $\beta$ O<sub>s</sub> exposure also induced ER stress, mainly by deregulating Ca<sup>+2</sup> levels [20]. Intracellular Ca<sup>+2</sup> deregulation has been considered an important event of damage associated with AD pathology progression [79]. Moreover, Ca<sup>+2</sup> is an ion that participates in the regulation of both tubulin and actin cytoskeleton polymerization [80,81]. On the other hand, Zhang and coworkers showed that in PC12 cells and primary neurons, A $\beta$ O<sub>s</sub> generated ER stress, JNK activation, and IRS-1 serine phosphorylation. This pathway contributes to Tau hyperphosphorylation, which causes

the disassembly of the tubulin cytoskeleton and neurofibrillary tangle formation [82]. Both of these changes play a major pathological role in AD.

Not only has ER rearrangement been associated with cytoskeleton modification, but it has also been proposed as a potential outcome of changes in its structural protein content. In this regard, we found that the level of calnexin expression, a type I integral ER membrane protein [83–85], did not change in SH-SY5Y cells after exposure to A $\beta$ O for 72 h, at least under our experimental conditions. This result indicates that even though A $\beta$ O generate ER rearrangement, this is not due to the decrease in calnexin protein expression. However, its modified distribution in the ER could be explained by the susceptibility of this protein to molecular modifications (e.g., phosphorylation or proteolytic cleavage) that cause changes in its localization, as previous studies have suggested [86–88]. Interestingly, different research groups have evidenced that A $\beta$  stimulation promotes the activation of kinases and caspases in cell cultures [89–91]. This could be the key to calnexin modification in the ER, although the precise mechanisms by which this change occurs and its connection with A $\beta$ O remain under investigation.

We also examined whether the arrangement of the GA would be altered in SH-SY5Y cells after A $\beta$ O exposure. In this regard, we found a significant dispersion of the GA in A $\beta$ O-exposed cells compared with non-exposed cells (Figure 5B,B1), suggesting that it is another effect of A $\beta$ O toxicity. Structural and functional alterations in the GA have been described in several neurodegenerative disorders including AD [92–94], demonstrating that the abnormal dispersion of this organelle has consequences that could be associated with the establishment of different pathologies. In AD, changes in the GA seem to be involved in ineffective protein transport through its membranes, causing the aberrant accumulation of proteins such as APP or Tau. This is a possible explanation for the dysfunction and subsequent cell death observed in this disease [95–97]. It has been demonstrated in brain tissue samples and experimental models of AD with A $\beta$  that the abnormal rearrangement of the GA affects cell morphology and several physiological functions [97–99]. It had been reported that A $\beta$  can alter the GA indirectly through the abnormal acetylation of cytoskeleton proteins, as well as by the induction of Tau hyperphosphorylation and cytoskeleton destabilization, which in turn disrupt intracellular transport [27,100,101]. Rodriguez-Cruz and collaborators recently reported similar data but using Tau protein overexpression as a pathological stimulus in SH-SY5Y cells. They showed that Tau protein indirectly produced GA dispersion, and the effects were associated with abnormal structural modifications of the tubulin cytoskeleton [102]. In light of these and other findings, it is not ruled out that there is a pathological relationship between the modification of the cytoskeleton and the disintegration of organelles like the ER and GA. However, this fact remains to be investigated.

Although GA rearrangement might be associated with cytoskeleton alterations, it is also probably linked to changes in its structural protein content caused by A $\beta$ O exposure. Golgin proteins located in the GA help to maintain its structure [103]. Therefore, disrupting these proteins leads to GA fragmentation or dispersion. In this study, we found evidence suggesting that A $\beta$ O generate GA rearrangement in SH-SY5Y cells, similar to what happens in the ER, but in this case a decrease in Golgin-97 protein expression seems to be involved (Figure 5C). Similar data were reported by Rodriguez-Cruz and collaborators. They found GA dispersion and reduced Golgin-97 expression in the SH-SY5Y cell line but using Tau protein overexpression as a pathological stimulus [102]. On the other hand, Giannopoulos and collaborators [104] demonstrated that, under A $\beta$  peptide incubation, the activity of cyclin-dependent kinase 5 (Cdk 5) increased, phosphorylating to Golgi matrix protein 130 (GM130), a protein located on the cis surface of the GA. GM130 is associated with GA structure regulation [105] and vesicle transport from the ER to GA [106], among other biological functions. Its phosphorylation causes abnormal GA destabilization and fragmentation [107]. It has been reported that GM130 inactivation occurs in patients with AD or other diseases [16,108]. An explanation for this is that GM130 deficits could generate an abnormal accumulation of proteins (e.g., Tau or APP) due to alterations in ER-to-Golgi

transport and sorting. Another report suggests that GRASP65, a peripheral protein that is located in the cis Golgi membranes and required for GA stacking, is phosphorylated by cdc2 due to the toxic effects of A $\beta$  peptide. This disrupts the oligomerization necessary to hold the Golgi membranes in stacks [107]. Interestingly, GM130 regulates the localization and stability of GRASP65 [109], increasing the pathological interest of these proteins in the disaggregation and dysfunction of the GA.

In summary, in this study we demonstrated that exposure to A $\beta$ Os in SH-SY5Y cells causes cell death, but the toxic effect is time-dependent, suggesting that this process could be slow and prolonged. Moreover, A $\beta$ O exposure causes an abnormal modification of tubulin and F-actin cytoskeleton distribution in survivor cells, suggesting that these organelles are sensitive to the toxic effects of A $\beta$ O at an early stage. In addition, A $\beta$ Os' toxic effects could mark the beginning of internal dysfunction and disorganization in the ER and GA. These alterations could be responsible for promoting ineffective post-translational protein processing, trafficking, and sorting, favoring an aberrant accumulation like that which occurs with Tau and A $\beta$ , common characteristics described in situ during the early stages of AD, hence its importance to continue be investigated. This study contributes to our understanding of the mechanism underlying the toxic effect of A $\beta$ Os on SH-SY5Y cells and suggests that the cytoskeleton and membranous organelles are susceptible to structural and functional alterations, although more research is needed to validate these findings.

**Author Contributions:** Conceptualization, J.J.J.-B. and Y.G.-M.; methodology, Y.G.-M.; validation, C.B.-Z., M.C.R.-C. and G.G.-C.; formal analysis, D.G.-M.; investigation, G.G.-C.; resources, G.G.-C.; writing—original draft preparation, J.J.J.-B.; visualization, N.J.C.-G.; supervision, M.C.R.-C. All authors have read and agreed to the published version of the manuscript.

**Funding:** This work was supported by the Guadalajara University program (Pro-SNI 2023 #270687 and p3e #267225) and program (Strengthening research #26962086, #271983).

**Institutional Review Board Statement:** Not applicable.

**Informed Consent Statement:** Not applicable.

**Data Availability Statement:** Data are contained within the article.

**Acknowledgments:** The authors thank Gabriela Escobar Camberos for the technical support.

**Conflicts of Interest:** The authors declare no conflicts of interest. The funders had no role in the design of the study; in the collection, analyses, or interpretation of data; in the writing of the manuscript; or in the decision to publish the results.

## References

1. Stakos, D.A.; Stamatelopoulos, K.; Bampatsias, D.; Sachse, M.; Zormpas, E.; Vlachogiannis, N.I.; Tual-Chalot, S.; Stellos, K. The alzheimer's disease amyloid-beta hypothesis in cardiovascular aging and disease: Jacc focus seminar. *J. Am. Coll. Cardiol.* **2020**, *75*, 952–967. [[CrossRef](#)] [[PubMed](#)]
2. Waigi, E.W.; Webb, R.C.; Moss, M.A.; Uline, M.J.; McCarthy, C.G.; Wenceslau, C.F. Soluble and insoluble protein aggregates, endoplasmic reticulum stress, and vascular dysfunction in alzheimer's disease and cardiovascular diseases. *Geroscience* **2023**, *45*, 1411–1438. [[CrossRef](#)] [[PubMed](#)]
3. Hampel, H.; Hardy, J.; Blennow, K.; Chen, C.; Perry, G.; Kim, S.H.; Villemagne, V.L.; Aisen, P.; Vendruscolo, M.; Iwatsubo, T.; et al. The amyloid-beta pathway in alzheimer's disease. *Mol. Psychiatry* **2021**, *26*, 5481–5503. [[CrossRef](#)]
4. Niewiadomska, G.; Niewiadomski, W.; Steczkowska, M.; Gasiorowska, A. Tau oligomers neurotoxicity. *Life* **2021**, *11*, 28. [[CrossRef](#)] [[PubMed](#)]
5. Vander Zanden, C.M.; Chi, E.Y. Passive immunotherapies targeting amyloid beta and tau oligomers in alzheimer's disease. *J. Pharm. Sci.* **2020**, *109*, 68–73. [[CrossRef](#)]
6. Gulisano, W.; Maugeri, D.; Baltrons, M.A.; Fa, M.; Amato, A.; Palmeri, A.; D'Adamio, L.; Grassi, C.; Devanand, D.P.; Honig, L.S.; et al. Role of amyloid-beta and tau proteins in alzheimer's disease: Confuting the amyloid cascade. *J. Alzheimers Dis.* **2018**, *64*, S611–S631. [[CrossRef](#)] [[PubMed](#)]
7. Carrillo-Mora, P.; Luna, R.; Colin-Barenque, L. Amyloid beta: Multiple mechanisms of toxicity and only some protective effects? *Oxid. Med. Cell Longev.* **2014**, *2014*, 795375. [[CrossRef](#)]
8. Shankar, G.M.; Walsh, D.M. Alzheimer's disease: Synaptic dysfunction and abeta. *Mol. Neurodegener.* **2009**, *4*, 48. [[CrossRef](#)]
9. Larson, M.E.; Lesne, S.E. Soluble abeta oligomer production and toxicity. *J. Neurochem.* **2012**, *120* (Suppl. S1), 125–139. [[CrossRef](#)]

10. Nimmrich, V.; Ebert, U. Is alzheimer's disease a result of presynaptic failure? Synaptic dysfunctions induced by oligomeric beta-amyloid. *Rev. Neurosci.* **2009**, *20*, 1–12. [[CrossRef](#)]
11. Qu, X.; Yuan, F.N.; Corona, C.; Pasini, S.; Pero, M.E.; Gundersen, G.G.; Shelanski, M.L.; Bartolini, F. Stabilization of dynamic microtubules by mdia1 drives tau-dependent abeta<sub>1-42</sub> synaptotoxicity. *J. Cell Biol.* **2017**, *216*, 3161–3178. [[CrossRef](#)] [[PubMed](#)]
12. Paradis, E.; Douillard, H.; Koutroumanis, M.; Goodyer, C.; LeBlanc, A. Amyloid beta peptide of alzheimer's disease downregulates bcl-2 and upregulates bax expression in human neurons. *J. Neurosci. Off. J. Soc. Neurosci.* **1996**, *16*, 7533–7539. [[CrossRef](#)] [[PubMed](#)]
13. Manczak, M.; Anekonda, T.S.; Henson, E.; Park, B.S.; Quinn, J.; Reddy, P.H. Mitochondria are a direct site of a beta accumulation in alzheimer's disease neurons: Implications for free radical generation and oxidative damage in disease progression. *Hum. Mol. Genet.* **2006**, *15*, 1437–1449. [[CrossRef](#)] [[PubMed](#)]
14. Reddy, P.H.; Manczak, M.; Mao, P.; Calkins, M.J.; Reddy, A.P.; Shirendeb, U. Amyloid-beta and mitochondria in aging and alzheimer's disease: Implications for synaptic damage and cognitive decline. *J. Alzheimer's Dis. JAD* **2010**, *20* (Suppl. S2), S499–S512. [[CrossRef](#)] [[PubMed](#)]
15. Ackerman, A.L.; Giodini, A.; Cresswell, P. A role for the endoplasmic reticulum protein retrotranslocation machinery during crosspresentation by dendritic cells. *Immunity* **2006**, *25*, 607–617. [[CrossRef](#)]
16. Stieber, A.; Mourelatos, Z.; Gonatas, N.K. In alzheimer's disease the golgi apparatus of a population of neurons without neurofibrillary tangles is fragmented and atrophic. *Am. J. Pathol.* **1996**, *148*, 415–426.
17. Ghanta, J.; Shen, C.L.; Kiessling, L.L.; Murphy, R.M. A strategy for designing inhibitors of beta-amyloid toxicity. *J. Biol. Chem.* **1996**, *271*, 29525–29528. [[CrossRef](#)] [[PubMed](#)]
18. Farquhar, M.G.; Palade, G.E. The golgi apparatus: 100 years of progress and controversy. *Trends Cell Biol.* **1998**, *8*, 2–10. [[CrossRef](#)]
19. Klein, W.L. Abeta toxicity in alzheimer's disease: Globular oligomers (addls) as new vaccine and drug targets. *Neurochem. Int.* **2002**, *41*, 345–352. [[CrossRef](#)]
20. Resende, R.; Ferreira, E.; Pereira, C.; Resende de Oliveira, C. Neurotoxic effect of oligomeric and fibrillar species of amyloid-beta peptide 1-42: Involvement of endoplasmic reticulum calcium release in oligomer-induced cell death. *Neuroscience* **2008**, *155*, 725–737. [[CrossRef](#)]
21. Picone, P.; Carrotta, R.; Montana, G.; Nobile, M.R.; San Biagio, P.L.; Di Carlo, M. Abeta oligomers and fibrillar aggregates induce different apoptotic pathways in lan5 neuroblastoma cell cultures. *Biophys. J.* **2009**, *96*, 4200–4211. [[CrossRef](#)] [[PubMed](#)]
22. Denizot, F.; Lang, R. Rapid colorimetric assay for cell growth and survival. Modifications to the tetrazolium dye procedure giving improved sensitivity and reliability. *J. Immunol. Methods* **1986**, *89*, 271–277. [[CrossRef](#)] [[PubMed](#)]
23. Tarozzi, A.; Merlicco, A.; Morroni, F.; Bolondi, C.; Di Iorio, P.; Ciccarelli, R.; Romano, S.; Giuliani, P.; Hrelia, P. Guanosine protects human neuroblastoma cells from oxidative stress and toxicity induced by amyloid-beta peptide oligomers. *J. Biol. Regul. Homeost. Agents* **2010**, *24*, 297–306.
24. Liu, L.; Zhang, C.; Kalionis, B.; Wan, W.; Murthi, P.; Chen, C.; Li, Y.; Xia, S. Egb761 protects against abeta<sub>1-42</sub> oligomer-induced cell damage via endoplasmic reticulum stress activation and hsp70 protein expression increase in sh-sy5y cells. *Exp. Gerontol.* **2016**, *75*, 56–63. [[CrossRef](#)]
25. de Medeiros, L.M.; De Bastiani, M.A.; Rico, E.P.; Schonhofen, P.; Pfaffenseller, B.; Wollenhaupt-Aguiar, B.; Grun, L.; Barbe-Tuana, F.; Zimmer, E.R.; Castro, M.A.A.; et al. Cholinergic differentiation of human neuroblastoma sh-sy5y cell line and its potential use as an in vitro model for alzheimer's disease studies. *Mol. Neurobiol.* **2019**, *56*, 7355–7367. [[CrossRef](#)] [[PubMed](#)]
26. Gomes, G.M.; Dalmolin, G.D.; Bar, J.; Karpova, A.; Mello, C.F.; Kreutz, M.R.; Rubin, M.A. Inhibition of the polyamine system counteracts beta-amyloid peptide-induced memory impairment in mice: Involvement of extrasynaptic nmda receptors. *PLoS ONE* **2014**, *9*, e99184. [[CrossRef](#)]
27. Fabbretti, E.; Antognolli, G.; Tongiorgi, E. Amyloid-beta impairs dendritic trafficking of golgi-like organelles in the early phase preceding neurite atrophy: Rescue by mirtazapine. *Front. Mol. Neurosci.* **2021**, *14*, 661728. [[CrossRef](#)]
28. SanMartin, C.D.; Veloso, P.; Adasme, T.; Lobos, P.; Bruna, B.; Galaz, J.; Garcia, A.; Hartel, S.; Hidalgo, C.; Paula-Lima, A.C. Ryr2-mediated Ca<sup>2+</sup> release and mitochondrial ros generation partake in the synaptic dysfunction caused by amyloid beta peptide oligomers. *Front. Mol. Neurosci.* **2017**, *10*, 115. [[CrossRef](#)]
29. Wang, L.; Cao, J.; Shi, Z.; Fan, W.; Liu, H.; Deng, J.; Deng, J. Experimental study on the neurotoxic effect of beta-amyloid on the cytoskeleton of pc12 cells. *Int. J. Mol. Med.* **2018**, *41*, 2764–2770.
30. Pchitskaya, E.; Rakovskaya, A.; Chigray, M.; Bezprozvanny, I. Cytoskeleton protein eb3 contributes to dendritic spines enlargement and enhances their resilience to toxic effects of beta-amyloid. *Int. J. Mol. Sci.* **2022**, *23*, 2274. [[CrossRef](#)]
31. Wu, J.C.; Liang, Z.Q.; Qin, Z.H. Quality control system of the endoplasmic reticulum and related diseases. *Acta Biochim. Biophys. Sin.* **2006**, *38*, 219–226. [[CrossRef](#)] [[PubMed](#)]
32. Siddiqi, M.K.; Malik, S.; Majid, N.; Alam, P.; Khan, R.H. Cytotoxic species in amyloid-associated diseases: Oligomers or mature fibrils. *Adv. Protein Chem. Struct. Biol.* **2019**, *118*, 333–369. [[PubMed](#)]
33. Pimplikar, S.W. Reassessing the amyloid cascade hypothesis of alzheimer's disease. *Int. J. Biochem. Cell Biol.* **2009**, *41*, 1261–1268. [[CrossRef](#)] [[PubMed](#)]
34. Morris, G.P.; Clark, I.A.; Vissel, B. Inconsistencies and controversies surrounding the amyloid hypothesis of alzheimer's disease. *Acta Neuropathol. Commun.* **2014**, *2*, 135. [[CrossRef](#)]

35. Toledo, J.P.; Fernandez-Perez, E.J.; Ferreira, I.L.; Marinho, D.; Riffo-Lepe, N.O.; Pineda-Cuevas, B.N.; Pinochet-Pino, L.F.; Burgos, C.F.; Rego, A.C.; Aguayo, L.G. Boldine attenuates synaptic failure and mitochondrial deregulation in cellular models of alzheimer's disease. *Front. Neurosci.* **2021**, *15*, 617821. [[CrossRef](#)]
36. Rudrabhatla, P. Regulation of neuronal cytoskeletal protein phosphorylation in neurodegenerative diseases. *J. Alzheimers Dis.* **2014**, *41*, 671–684. [[CrossRef](#)] [[PubMed](#)]
37. Huang, H.C.; Tang, D.; Lu, S.Y.; Jiang, Z.F. Endoplasmic reticulum stress as a novel neuronal mediator in alzheimer's disease. *Neurol. Res.* **2015**, *37*, 366–374. [[CrossRef](#)]
38. Narayan, P.; Krishnarajuna, B.; Vishwanathan, V.; Jagadeesh Kumar, D.; Babu, S.; Ramanathan, K.V.; Easwaran, K.R.; Nagendra, H.G.; Raghobhama, S. Does aluminium bind to histidine? An nmr investigation of amyloid beta12 and amyloid beta16 fragments. *Chem. Biol. Drug Des.* **2013**, *82*, 48–59. [[CrossRef](#)] [[PubMed](#)]
39. Nelson, P.T.; Abner, E.L.; Schmitt, F.A.; Kryscio, R.J.; Jicha, G.A.; Santacruz, K.; Smith, C.D.; Patel, E.; Markesbery, W.R. Brains with medial temporal lobe neurofibrillary tangles but no neuritic amyloid plaques are a diagnostic dilemma but may have pathogenetic aspects distinct from alzheimer disease. *J. Neuropathol. Exp. Neurol.* **2009**, *68*, 774–784. [[CrossRef](#)]
40. Malaplate-Armand, C.; Florent-Bechard, S.; Youssef, I.; Koziel, V.; Sponne, I.; Kriem, B.; Leininger-Muller, B.; Olivier, J.L.; Oster, T.; Pillot, T. Soluble oligomers of amyloid-beta peptide induce neuronal apoptosis by activating a cpla2-dependent sphingomyelinase-ceramide pathway. *Neurobiol. Dis.* **2006**, *23*, 178–189. [[CrossRef](#)]
41. Monroy-Ramirez, H.C.; Basurto-Islas, G.; Mena, R.; Cisneros, B.; Binder, L.I.; Avila, J.; Garcia-Sierra, F. Alterations in the nuclear architecture produced by the overexpression of tau protein in neuroblastoma cells. *J. Alzheimers Dis.* **2013**, *36*, 503–520. [[CrossRef](#)] [[PubMed](#)]
42. Braak, H.; Braak, E. Neuropathological staging of alzheimer-related changes. *Acta Neuropathol.* **1991**, *82*, 239–259. [[CrossRef](#)] [[PubMed](#)]
43. Selkoe, D.J. Alzheimer's disease is a synaptic failure. *Science* **2002**, *298*, 789–791. [[CrossRef](#)] [[PubMed](#)]
44. Guerrero-Munoz, M.J.; Gerson, J.; Castillo-Carranza, D.L. Tau oligomers: The toxic player at synapses in alzheimer's disease. *Front. Cell Neurosci.* **2015**, *9*, 464. [[CrossRef](#)] [[PubMed](#)]
45. Tsai, J.; Grutzendler, J.; Duff, K.; Gan, W.B. Fibrillar amyloid deposition leads to local synaptic abnormalities and breakage of neuronal branches. *Nat. Neurosci.* **2004**, *7*, 1181–1183. [[CrossRef](#)] [[PubMed](#)]
46. Ripoli, C.; Piacentini, R.; Riccardi, E.; Leone, L.; Li Puma, D.D.; Bitan, G.; Grassi, C. Effects of different amyloid beta-protein analogues on synaptic function. *Neurobiol. Aging* **2013**, *34*, 1032–1044. [[CrossRef](#)]
47. Lasagna-Reeves, C.A.; Castillo-Carranza, D.L.; Sengupta, U.; Clos, A.L.; Jackson, G.R.; Kaye, R. Tau oligomers impair memory and induce synaptic and mitochondrial dysfunction in wild-type mice. *Mol. Neurodegener.* **2011**, *6*, 39. [[CrossRef](#)]
48. Fa, M.; Puzzo, D.; Piacentini, R.; Staniszewski, A.; Zhang, H.; Baltrons, M.A.; Li Puma, D.D.; Chatterjee, I.; Li, J.; Saeed, F.; et al. Extracellular tau oligomers produce an immediate impairment of ltp and memory. *Sci. Rep.* **2016**, *6*, 19393. [[CrossRef](#)]
49. Calingasan, N.Y.; Chen, J.; Kiaei, M.; Beal, M.F. Beta-amyloid 42 accumulation in the lumbar spinal cord motor neurons of amyotrophic lateral sclerosis patients. *Neurobiol. Dis.* **2005**, *19*, 340–347. [[CrossRef](#)]
50. Green, K.N.; Steffan, J.S.; Martinez-Coria, H.; Sun, X.; Schreiber, S.S.; Thompson, L.M.; LaFerla, F.M. Nicotinamide restores cognition in alzheimer's disease transgenic mice via a mechanism involving sirtuin inhibition and selective reduction of thr231-phosphotau. *J. Neurosci. Off. J. Soc. Neurosci.* **2008**, *28*, 11500–11510. [[CrossRef](#)]
51. Pianu, B.; Lefort, R.; Thuiliere, L.; Tabourier, E.; Bartolini, F. The abeta<sub>1-42</sub> peptide regulates microtubule stability independently of tau. *J. Cell Sci.* **2014**, *127*, 1117–1127. [[PubMed](#)]
52. Torres-Cruz, F.M.; Rodriguez-Cruz, F.; Escobar-Herrera, J.; Barragan-Andrade, N.; Basurto-Islas, G.; Ripova, D.; Avila, J.; Garcia-Sierra, F. Expression of tau produces aberrant plasma membrane blebbing in glial cells through rhoa-rock-dependent f-actin remodeling. *J. Alzheimers Dis.* **2016**, *52*, 463–482. [[CrossRef](#)] [[PubMed](#)]
53. Yoshiyama, Y.; Zhang, B.; Bruce, J.; Trojanowski, J.Q.; Lee, V.M. Reduction of detyrosinated microtubules and golgi fragmentation are linked to tau-induced degeneration in astrocytes. *J. Neurosci.* **2003**, *23*, 10662–10671. [[CrossRef](#)] [[PubMed](#)]
54. Chesarone, M.A.; DuPage, A.G.; Goode, B.L. Unleashing formins to remodel the actin and microtubule cytoskeletons. *Nat. Rev. Mol. Cell Biol.* **2010**, *11*, 62–74. [[CrossRef](#)] [[PubMed](#)]
55. Yamana, N.; Arakawa, Y.; Nishino, T.; Kurokawa, K.; Tanji, M.; Itoh, R.E.; Monypenny, J.; Ishizaki, T.; Bito, H.; Nozaki, K.; et al. The rho-mdial1 pathway regulates cell polarity and focal adhesion turnover in migrating cells through mobilizing apc and c-src. *Mol. Cell. Biol.* **2006**, *26*, 6844–6858. [[CrossRef](#)]
56. Hotulainen, P.; Llano, O.; Smirnov, S.; Tanhuanpaa, K.; Faix, J.; Rivera, C.; Lappalainen, P. Defining mechanisms of actin polymerization and depolymerization during dendritic spine morphogenesis. *J. Cell Biol.* **2009**, *185*, 323–339. [[CrossRef](#)] [[PubMed](#)]
57. Mishra, M.; Huang, J.; Balasubramanian, M.K. The yeast actin cytoskeleton. *FEMS Microbiol. Rev.* **2014**, *38*, 213–227. [[CrossRef](#)] [[PubMed](#)]
58. Ma, Q.L.; Yang, F.; Calon, F.; Ubeda, O.J.; Hansen, J.E.; Weisbart, R.H.; Beech, W.; Frautschy, S.A.; Cole, G.M. P21-activated kinase-aberrant activation and translocation in alzheimer disease pathogenesis. *J. Biol. Chem.* **2008**, *283*, 14132–14143. [[PubMed](#)]
59. Nam, K.N.; Mounier, A.; Wolfe, C.M.; Fitz, N.F.; Carter, A.Y.; Castranio, E.L.; Kamboh, H.I.; Reeves, V.L.; Wang, J.; Han, X.; et al. Effect of high fat diet on phenotype, brain transcriptome and lipidome in alzheimer's model mice. *Sci. Rep.* **2017**, *7*, 4307. [[CrossRef](#)]

60. Popugaeva, E.; Bezprozvanny, I. Role of endoplasmic reticulum  $ca^{2+}$  signaling in the pathogenesis of alzheimer disease. *Front. Mol. Neurosci.* **2013**, *6*, 29. [[CrossRef](#)]
61. Saito, T.; Matsuba, Y.; Mihira, N.; Takano, J.; Nilsson, P.; Itohara, S.; Iwata, N.; Saido, T.C. Single app knock-in mouse models of alzheimer's disease. *Nat. Neurosci.* **2014**, *17*, 661–663. [[PubMed](#)]
62. Aihara, Y.; Inoue, T.; Tashiro, T.; Okamoto, K.; Komiya, Y.; Mikoshiba, K. Movement of endoplasmic reticulum in the living axon is distinct from other membranous vesicles in its rate, form, and sensitivity to microtubule inhibitors. *J. Neurosci. Res.* **2001**, *65*, 236–246. [[CrossRef](#)] [[PubMed](#)]
63. Bannai, H.; Inoue, T.; Nakayama, T.; Hattori, M.; Mikoshiba, K. Kinesin dependent, rapid, bi-directional transport of er sub-compartment in dendrites of hippocampal neurons. *J. Cell Sci.* **2004**, *117*, 163–175. [[CrossRef](#)] [[PubMed](#)]
64. Chaudhari, N.; Talwar, P.; Parimisetty, A.; Lefebvre d'Helencourt, C.; Ravanan, P. A molecular web: Endoplasmic reticulum stress, inflammation, and oxidative stress. *Front. Cell Neurosci.* **2014**, *8*, 213. [[CrossRef](#)] [[PubMed](#)]
65. Hetz, C.; Mollereau, B. Disturbance of endoplasmic reticulum proteostasis in neurodegenerative diseases. *Nat. Rev. Neurosci.* **2014**, *15*, 233–249. [[CrossRef](#)] [[PubMed](#)]
66. Chiti, F.; Dobson, C.M. Protein misfolding, amyloid formation, and human disease: A summary of progress over the last decade. *Annu. Rev. Biochem.* **2017**, *86*, 27–68. [[CrossRef](#)] [[PubMed](#)]
67. Sengupta, U.; Nilson, A.N.; Kaye, R. The role of amyloid-beta oligomers in toxicity, propagation, and immunotherapy. *EBioMedicine* **2016**, *6*, 42–49. [[CrossRef](#)] [[PubMed](#)]
68. Hartmann, T.; Bieger, S.C.; Bruhl, B.; Tienari, P.J.; Ida, N.; Allsop, D.; Roberts, G.W.; Masters, C.L.; Dotti, C.G.; Unsicker, K.; et al. Distinct sites of intracellular production for alzheimer's disease a beta40/42 amyloid peptides. *Nat. Med.* **1997**, *3*, 1016–1020. [[CrossRef](#)] [[PubMed](#)]
69. Jung, E.S.; Hong, H.; Kim, C.; Mook-Jung, I. Acute er stress regulates amyloid precursor protein processing through ubiquitin-dependent degradation. *Sci. Rep.* **2015**, *5*, 8805. [[CrossRef](#)]
70. Sakono, M.; Zako, T. Amyloid oligomers: Formation and toxicity of abeta oligomers. *FEBS J.* **2010**, *277*, 1348–1358. [[CrossRef](#)]
71. Gorbatyuk, M.S.; Gorbatyuk, O.S. The molecular chaperone grp78/bip as a therapeutic target for neurodegenerative disorders: A mini review. *J. Genet. Syndr. Gene Ther.* **2013**, *4*, 128. [[CrossRef](#)] [[PubMed](#)]
72. Nagele, R.G.; D'Andrea, M.R.; Anderson, W.J.; Wang, H.Y. Intracellular accumulation of beta-amyloid<sub>1-42</sub> in neurons is facilitated by the alpha 7 nicotinic acetylcholine receptor in alzheimer's disease. *Neuroscience* **2002**, *110*, 199–211. [[CrossRef](#)]
73. Shankar, G.M.; Li, S.; Mehta, T.H.; Garcia-Munoz, A.; Shepardson, N.E.; Smith, I.; Brett, F.M.; Farrell, M.A.; Rowan, M.J.; Lemere, C.A.; et al. Amyloid-beta protein dimers isolated directly from alzheimer's brains impair synaptic plasticity and memory. *Nat. Med.* **2008**, *14*, 837–842. [[CrossRef](#)]
74. Musiek, E.S.; Holtzman, D.M. Three dimensions of the amyloid hypothesis: Time, space and 'wingmen'. *Nat. Neurosci.* **2015**, *18*, 800–806. [[CrossRef](#)]
75. Lee, S.J.; Nam, E.; Lee, H.J.; Savelieff, M.G.; Lim, M.H. Towards an understanding of amyloid-beta oligomers: Characterization, toxicity mechanisms, and inhibitors. *Chem. Soc. Rev.* **2017**, *46*, 310–323. [[CrossRef](#)]
76. Ferreira, I.L.; Ferreira, E.; Schmidt, J.; Cardoso, J.M.; Pereira, C.M.; Carvalho, A.L.; Oliveira, C.R.; Rego, A.C. Abeta and nmdar activation cause mitochondrial dysfunction involving er calcium release. *Neurobiol. Aging* **2015**, *36*, 680–692. [[CrossRef](#)] [[PubMed](#)]
77. Stefani, I.C.; Wright, D.; Polizzi, K.M.; Kontoravdi, C. The role of er stress-induced apoptosis in neurodegeneration. *Curr. Alzheimer Res.* **2012**, *9*, 373–387. [[CrossRef](#)]
78. Pannaccione, A.; Secondo, A.; Molinaro, P.; D'Avanzo, C.; Cantile, M.; Esposito, A.; Boscia, F.; Scorziello, A.; Sirabella, R.; Sokolow, S.; et al. A new concept: Abeta1-42 generates a hyperfunctional proteolytic ncx3 fragment that delays caspase-12 activation and neuronal death. *J. Neurosci.* **2012**, *32*, 10609–10617. [[CrossRef](#)] [[PubMed](#)]
79. Mota, S.I.; Ferreira, I.L.; Pereira, C.; Oliveira, C.R.; Rego, A.C. Amyloid-beta peptide 1-42 causes microtubule deregulation through n-methyl-d-aspartate receptors in mature hippocampal cultures. *Curr. Alzheimer Res.* **2012**, *9*, 844–856. [[CrossRef](#)]
80. Merriam, E.B.; Millette, M.; Lumbard, D.C.; Saengsawang, W.; Fothergill, T.; Hu, X.; Ferhat, L.; Dent, E.W. Synaptic regulation of microtubule dynamics in dendritic spines by calcium, f-actin, and drebrin. *J. Neurosci.* **2013**, *33*, 16471–16482. [[CrossRef](#)]
81. Sergeeva, M.; Ubl, J.J.; Reiser, G. Disruption of actin cytoskeleton in cultured rat astrocytes suppresses atp- and bradykinin-induced  $[Ca^{2+}]_i$  oscillations by reducing the coupling efficiency between  $Ca^{2+}$  release, capacitative  $Ca^{2+}$  entry, and store refilling. *Neuroscience* **2000**, *97*, 765–769. [[CrossRef](#)] [[PubMed](#)]
82. Zhang, X.; Tang, S.; Zhang, Q.; Shao, W.; Han, X.; Wang, Y.; Du, Y. Endoplasmic reticulum stress mediates jnk-dependent irs-1 serine phosphorylation and results in tau hyperphosphorylation in amyloid beta oligomer-treated pc12 cells and primary neurons. *Gene* **2016**, *587*, 183–193. [[CrossRef](#)]
83. Li, H.D.; Liu, W.X.; Michalak, M. Enhanced clathrin-dependent endocytosis in the absence of calnexin. *PLoS ONE* **2011**, *6*, e21678. [[CrossRef](#)] [[PubMed](#)]
84. Gutierrez, T.; Qi, H.; Yap, M.C.; Tahbaz, N.; Milburn, L.A.; Lucchinetti, E.; Lou, P.H.; Zaugg, M.; LaPointe, P.G.; Mercier, P.; et al. The er chaperone calnexin controls mitochondrial positioning and respiration. *Sci. Signal* **2020**, *13*, eaax6660. [[CrossRef](#)] [[PubMed](#)]
85. Paskevicius, T.; Farraj, R.A.; Michalak, M.; Agellon, L.B. Calnexin, more than just a molecular chaperone. *Cells* **2023**, *12*, 403. [[CrossRef](#)]
86. Lakkaraju, A.K.; van der Goot, F.G. Calnexin controls the stat3-mediated transcriptional response to egf. *Mol. Cell* **2013**, *51*, 386–396. [[CrossRef](#)] [[PubMed](#)]

87. Chevet, E.; Wong, H.N.; Gerber, D.; Cochet, C.; Fazel, A.; Cameron, P.H.; Gushue, J.N.; Thomas, D.Y.; Bergeron, J.J. Phosphorylation by ck2 and mapk enhances calnexin association with ribosomes. *EMBO J.* **1999**, *18*, 3655–3666. [[CrossRef](#)]
88. Cameron, P.H.; Chevet, E.; Pluquet, O.; Thomas, D.Y.; Bergeron, J.J. Calnexin phosphorylation attenuates the release of partially misfolded alpha1-antitrypsin to the secretory pathway. *J. Biol. Chem.* **2009**, *284*, 34570–34579. [[CrossRef](#)]
89. Ontiveros-Torres, M.A.; Labra-Barrios, M.L.; Diaz-Cintra, S.; Aguilar-Vazquez, A.R.; Moreno-Campuzano, S.; Flores-Rodriguez, P.; Luna-Herrera, C.; Mena, R.; Perry, G.; Floran-Garduno, B.; et al. Fibrillar amyloid-beta accumulation triggers an inflammatory mechanism leading to hyperphosphorylation of the carboxyl-terminal end of tau polypeptide in the hippocampal formation of the 3xtg-ad transgenic mouse. *J. Alzheimers Dis.* **2016**, *52*, 243–269. [[CrossRef](#)]
90. Troy, C.M.; Rabacchi, S.A.; Friedman, W.J.; Frappier, T.F.; Brown, K.; Shelanski, M.L. Caspase-2 mediates neuronal cell death induced by beta-amyloid. *J. Neurosci.* **2000**, *20*, 1386–1392. [[CrossRef](#)]
91. Gamblin, T.C.; Chen, F.; Zambrano, A.; Abraha, A.; Lagalwar, S.; Guillozet, A.L.; Lu, M.; Fu, Y.; Garcia-Sierra, F.; LaPointe, N.; et al. Caspase cleavage of tau: Linking amyloid and neurofibrillary tangles in alzheimer's disease. *Proc. Natl. Acad. Sci. USA* **2003**, *100*, 10032–10037. [[CrossRef](#)] [[PubMed](#)]
92. Ayala, I.; Colanzi, A. Alterations of golgi organization in alzheimer's disease: A cause or a consequence? *Tissue Cell* **2017**, *49*, 133–140. [[CrossRef](#)] [[PubMed](#)]
93. Martinez-Menarguez, J.A.; Tomas, M.; Martinez-Martinez, N.; Martinez-Alonso, E. Golgi fragmentation in neurodegenerative diseases: Is there a common cause? *Cells* **2019**, *8*, 748. [[CrossRef](#)] [[PubMed](#)]
94. Jungk, L.; Franke, H.; Salameh, A.; Dhein, S. Golgi fragmentation in human patients with chronic atrial fibrillation: A new aspect of remodeling. *Thorac. Cardiovasc. Surg.* **2019**, *67*, 98–106. [[CrossRef](#)]
95. Kinoshita, A.; Fukumoto, H.; Shah, T.; Whelan, C.M.; Irizarry, M.C.; Hyman, B.T. Demonstration by fret of bace interaction with the amyloid precursor protein at the cell surface and in early endosomes. *J. Cell Sci.* **2003**, *116*, 3339–3346. [[CrossRef](#)] [[PubMed](#)]
96. Joshi, G.; Wang, Y. Golgi defects enhance app amyloidogenic processing in alzheimer's disease. *Bioessays* **2015**, *37*, 240–247. [[CrossRef](#)]
97. Anton-Fernandez, A.; Merchan-Rubira, J.; Avila, J.; Hernandez, F.; DeFelipe, J.; Munoz, A. Phospho-tau accumulation and structural alterations of the golgi apparatus of cortical pyramidal neurons in the p301s tauopathy mouse model. *J. Alzheimers Dis.* **2017**, *60*, 651–661. [[CrossRef](#)] [[PubMed](#)]
98. Baloyannis, S.J. Golgi apparatus and protein trafficking in alzheimer's disease. *J. Alzheimers Dis.* **2014**, *42* (Suppl. S3), S153–S162. [[CrossRef](#)]
99. Cole, N.B.; Sciaky, N.; Marotta, A.; Song, J.; Lippincott-Schwartz, J. Golgi dispersal during microtubule disruption: Regeneration of golgi stacks at peripheral endoplasmic reticulum exit sites. *Mol. Biol. Cell* **1996**, *7*, 631–650. [[CrossRef](#)]
100. Ballatore, C.; Lee, V.M.; Trojanowski, J.Q. Tau-mediated neurodegeneration in alzheimer's disease and related disorders. *Nat. Rev. Neurosci.* **2007**, *8*, 663–672. [[CrossRef](#)]
101. Cohen, T.J.; Guo, J.L.; Hurtado, D.E.; Kwong, L.K.; Mills, I.P.; Trojanowski, J.Q.; Lee, V.M. The acetylation of tau inhibits its function and promotes pathological tau aggregation. *Nat. Commun.* **2011**, *2*, 252. [[CrossRef](#)] [[PubMed](#)]
102. Rodriguez-Cruz, F.; Torres-Cruz, F.M.; Monroy-Ramirez, H.C.; Escobar-Herrera, J.; Basurto-Islas, G.; Avila, J.; Garcia-Sierra, F. Fragmentation of the golgi apparatus in neuroblastoma cells is associated with tau-induced ring-shaped microtubule bundles. *J. Alzheimers Dis.* **2018**, *65*, 1185–1207. [[CrossRef](#)] [[PubMed](#)]
103. Lu, L.; Tai, G.; Hong, W. Autoantigen golgin-97, an effector of arl1 gtpase, participates in traffic from the endosome to the trans-golgi network. *Mol. Biol. Cell* **2004**, *15*, 4426–4443. [[CrossRef](#)]
104. Giannopoulos, P.F.; Joshi, Y.B.; Pratico, D. Novel lipid signaling pathways in alzheimer's disease pathogenesis. *Biochem. Pharmacol.* **2014**, *88*, 560–564. [[CrossRef](#)] [[PubMed](#)]
105. Nakamura, N.; Rabouille, C.; Watson, R.; Nilsson, T.; Hui, N.; Slusarewicz, P.; Kreis, T.E.; Warren, G. Characterization of a cis-golgi matrix protein, gm130. *J. Cell Biol.* **1995**, *131*, 1715–1726. [[CrossRef](#)] [[PubMed](#)]
106. Marra, P.; Salvatore, L.; Mironov, A., Jr.; Di Campli, A.; Di Tullio, G.; Trucco, A.; Beznoussenko, G.; Mironov, A.; De Matteis, M.A. The biogenesis of the golgi ribbon: The roles of membrane input from the er and of gm130. *Mol. Biol. Cell* **2007**, *18*, 1595–1608. [[CrossRef](#)] [[PubMed](#)]
107. Sun, K.H.; de Pablo, Y.; Vincent, F.; Johnson, E.O.; Chavers, A.K.; Shah, K. Novel genetic tools reveal cdk5's major role in golgi fragmentation in alzheimer's disease. *Mol. Biol. Cell* **2008**, *19*, 3052–3069. [[CrossRef](#)] [[PubMed](#)]
108. Huang, B.; Li, X.; Zhu, X. The role of gm130 in nervous system diseases. *Front. Neurol.* **2021**, *12*, 743787. [[CrossRef](#)]
109. Puthenveedu, M.A.; Bachert, C.; Puri, S.; Lanni, F.; Linstedt, A.D. Gm130 and grasp65-dependent lateral cisternal fusion allows uniform golgi-enzyme distribution. *Nat. Cell Biol.* **2006**, *8*, 238–248. [[CrossRef](#)]

**Disclaimer/Publisher's Note:** The statements, opinions and data contained in all publications are solely those of the individual author(s) and contributor(s) and not of MDPI and/or the editor(s). MDPI and/or the editor(s) disclaim responsibility for any injury to people or property resulting from any ideas, methods, instructions or products referred to in the content.